Electronic Supplementary Material (ESI) for Sustainable Energy & Fuels.

Supplementary Information

Reaping the catalytic benefits of both surface ($NiFe_2O_4$) and underneath (Ni_3Fe) layers for the oxygen evolution reaction

Mohammad Alharthy,[a] Munzir H. Suliman,[a,b] Abdul-Rahman Al-Betar,[a] Yuan Wang,[c] Ziqi Tian,[c] Qasem A. Drmosh,[b] Zain H. Yamani,[b] Mohammad Qamar,[b,d*]

[a]Department of Chemistry, [b]Center of Excellence in Nanotechnology (CENT), King Fahd University of Petroleum and Minerals, Dhahran 31261, Saudi Arabia.

[c]Ningbo Institute of Materials Technology and Engineering, Chinese Academy of Sciences, 1219 Zhongguan West Road, Ningbo 315201, Zhejiang, P. R. China.

[d]K.A.CARE Energy Research & Innovation Center, King Fahd University of Petroleum and Minerals, Dhahran 31261, Saudi Arabia.

*Corresponding author – qamar@kfupm.edu.sa

Experimental

Materials

Hydrochloric acid (37%), Potassium persulfate (99.99% trace metals basis), aniline, (Nickel (II) acetate tetrahydrate (≥99.5%), Iron (III) acetylacetonate (97%), Benzyl alcohol (99.8%), acetone (≥99.5%), and anhydrous ethanol were purchased from Sigma-Aldrich, while Nafion (5% w/w solution) was obtained from Alfa Aesar.

Synthesis of Polyaniline (PANI)

PANI was prepared by oxidative polymerization. Two solutions were prepared by adding 0.5 mL of aniline and 1.55 g of potassium persulfate ($K_2S_2O_8$) each into 50 mL of 1.0 M hydrochloric acid (HCl). Then, the two solutions were mixed together, and the reaction was allowed to take place. Polymerization of aniline or formation of PANI was indicated by the change in color. After 7 min, the reaction was terminated by the addition of 10 mL of water. Finally, the formed precipitate (PANI) was filtered out from the solution using gravity filtration and dried at 90 °C for 4 h.

Characterization

Morphological and detailed microstructural attributes of the materials were discerned with the aid of field emission scanning electron microscope (FESEM), transmission and high-resolution transmission electron microscope and selected area electron diffraction (TEM/HR-TEM, FEI Tecnai TF20) (SAED). Other techniques employed for characterization of the samples were: X-ray diffractometry (XRD, Rigaku MiniFlex), X-ray photoelectron spectroscopy (XPS, Thermo Scientific ESCALAB 250Xi).

Electrocatalytic performance evaluation

The performance was evaluated in a three-electrode cell configuration connected to a potentiostat (EG&G 273A) at ambient conditions. Working electrode was prepared sonicating (~ 30 min) the slurry consisting of electrocatalyst (2 mg) and 1 ml mixture of 630 µl deionized water, 330 µl ethanol and 40 µl Nafion (1.66%). 6.0 µL of sonicated solution was dropped on a pre-cleaned glassy carbon (GC) disc electrode (0.196 mm diameter), and dried under ambient conditions. Saturated calomel electrode ($Hg/HgCl_2$, SCE) and graphite rod were used as the reference and the counter electrode, respectively. The SCE

potential was measured experimentally, converted and presented against reversible hydrogen electrode (RHE). Linear sweep voltammetry was performed in a 1.0 M KOH aqueous solution at a scan rate of 5 mV s^{-1}. All current density was normalized to the geometric area of the glassy carbon electrode, unless stated otherwise, and presented after *iR* compensation. Electrochemical impedance spectroscopy (EIS) measurements were carried out in 1.0 M KOH between the frequency range of 10^5 Hz and 0.01 Hz with ac amplitude of 10 mV. All the EIS data was normalized to the geometric area of the working electrode.

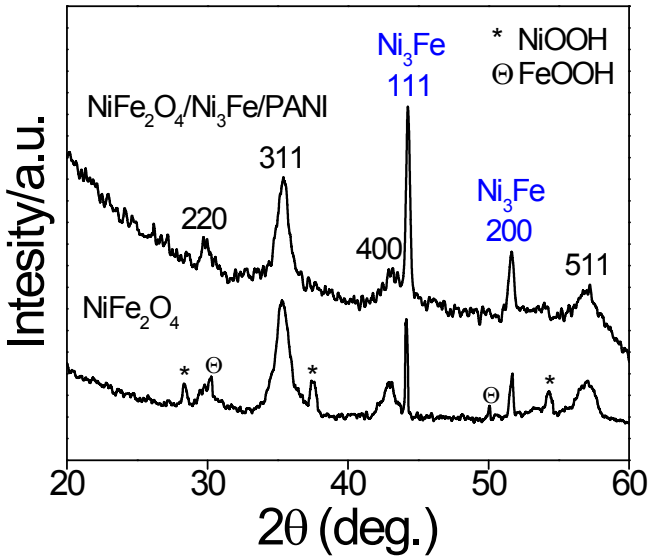

Fig. S1 Powder XRD of $NiFe_2O_4/Ni_3Fe$/PANI before and after the stability test.

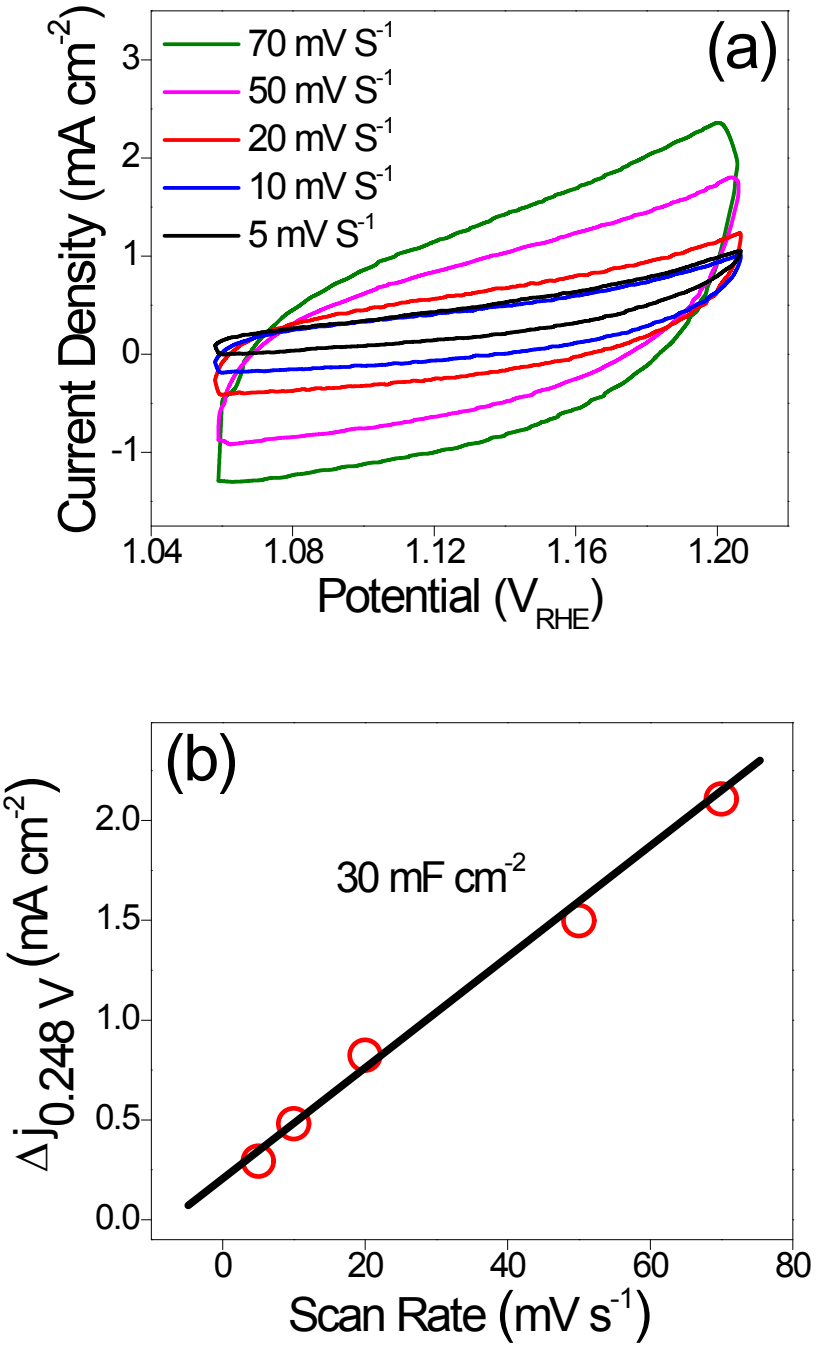

Fig. S2 Cyclic voltammetry (a) and corresponding slopes (b) of $NiFe_2O_4$.

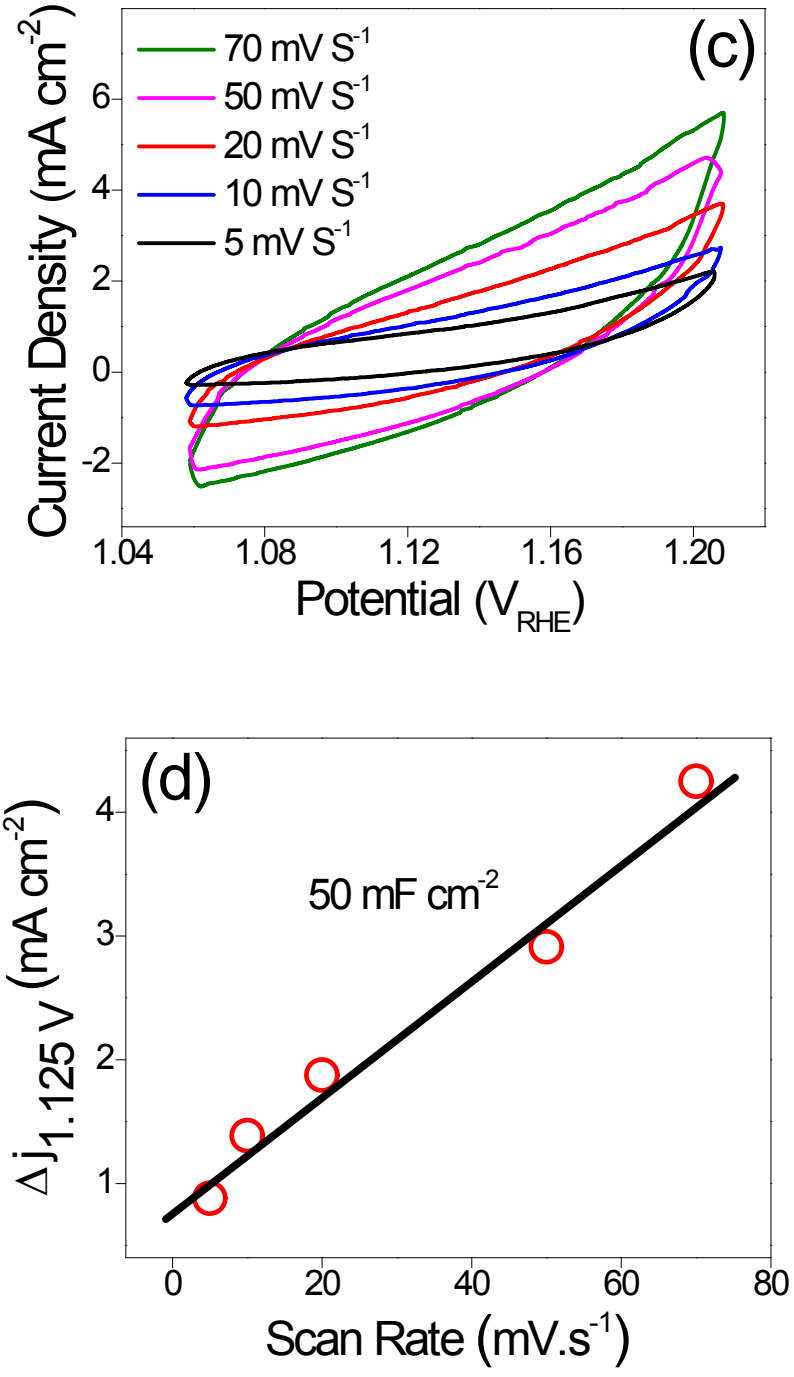

Fig. S3 Cyclic voltammetry (c) and corresponding slopes (d) of $NiFe_2O_4/Ni_3Fe/PANI$.

Table S1. The OER activity comparison of the $NiFe_2O_4/Ni_3Fe$/PANI with some advanced transition metal-based electrocatalysts.

Electrocatalyst	η_{10}	Tafel slope (mV dec^{-1})	Electrolyte	Reference
α-$Ni(OH)_2$ hollow nanospheres	331	42	0.1 M KOH	1
$NiFe_2O_4$ nanofiber	390	60	1.0 M KOH	2
Amorphous $Ni(OH)_2$ nanosheets/graphite	344	46	0.1 M KOH	3
NiCoFe LDH nanoplates	340	93	0.1 M KOH	4
NiCo LDH nanosheets	420	113	0.1 M KOH	5
$CoFe_2O_4$ nanoparticles	360	54.7	1.0 M KOH	6
$CoFe_2O_4$/MWCNT	345	38.1	1.0 M KOH	6
$CoFe_2O_4$/PANI-MWCNTs	314	30.7	1.0 M KOH	6
Mesoporous $NiFe_2O_4$ nanorods	342	44	1.0 M KOH	7
FeNi/$NiFe_2O_4$/CN	316	60	1.0 M KOH	8
Benzoate ion intercalated $Co(OH)_2$	360	76	1.0 M KOH	9
Mesoporous NiO/MnO_2/PANI	345	42	6.0 M KOH	10
β-$Ni(OH)_2/Cu_2S$ hybrid nanosheets	500	89	0.1 M KOH	11
Fe-CoOOH/Graphene	330	37	1.0 M KOH	12
NC-NiFeS with defects	350	93	1.0 M KOH	13
NiF-O with metal vacancies	371	28	1.0 M KOH	14
NiO	445	34	1.0 M KOH	14
Co-Fe double atom catalyst	309	37	1.0 M KOH	15
$(Co/Fe)_4O_4$	300	36	1.0 M KOH	16
Fe/BIF-91(Co)	350	71	1.0 M KOH	17
$NiFe_2O_4$ nanoparticles	500	122	1.0 M KOH	18
Fe-NiNC	340	54	1.0 M KOH	19
FeNi/graphene	380	75	1.0 M KOH	20
Fe-Nx-S/C	326	42	1.0 M KOH	21
$Ni_3Fe/NiFe_2O_4$/PANI	320	52	1.0 M KOH	This Work

References

1 M. Gao, W. Sheng, Z. Zhuang, Q. Fang, S. Gu, J. Jiang and Y. Yan, *J. Am. Chem. Soc.,* 2014, **136**, 7077–7084.

2 Z. Peng, D. Jia, A.M. Al-Enizi, A.A. Elzatahry and G. Zheng, *Adv. Energ. Mater.*, 2015, **5**, 1402031.

3 Y. Gao, H. Li and G. Yang, *Cryst. Growth Des.*, 2015, **15**, 4475.

4 L. Qian, Z. Lu, T. Xu, X. Wu, Y. Tian, Y. Li, Z. Huo, X. Sun and X. Duan, *Adv. Energy Mater.*, 2015, **5**, 1500245.

5 J. Jiang, A. Zhang, L. Li and L. Ai, *J. Power Sources*, 2015, **278**, 445.

6 Y. Liu, J. Li, F. Li, W. Li, H. Yang, X. Zhang, Y. Liu and J. Ma, *J. Mater. Chem. A*, 2016, **4**, 4472–4478.

7 G. Liu, K. Wang, X. Gao, D. He and J. Li, *Electrochim. Acta*, 2016, **211**, 871−878.

8 Y. Ma, X. Dai, M. Liu, J. Yong, H. Qiao, A. Jin, Z. Li, X. Huang, H. Wang and X. Zhang, *ACS Appl. Mater. Interfaces*, 2016, **8**, 34396-34404.

9 L. Tao, C.-Y. Lin, S. Dou, S. Feng, D. Chen, D. Liu, J. Huo, Z. Xia and S. Wang, *Nano Energy*, 2017, **41**, 417-425.

10 J. He, M. Wang, W. Wang, R. Miao, W. Zhong, S.-Y. Chen, S. Poges, T. Jafari, W. Song, J. Liu and S.L. Suib, *ACS Appl. Mater. Interfaces*, 2017, **9**, 42676−42687.

11 D. Yang, L. Gao and J.-H. Yang, *J. Power Sources*, 2017, **359**, 52-56.

12 X. Han, C, Yu, S. Zhou, C. Zhao, H. Huang, J. Yang, Z. Liu, J. Zhao and J. Qiu. *Adv. Energy Mater.*, 2017, **7**, 1602148.

13 C. Han, W. Li, C. Shu, H. Guo, H. Liu, S. Dou and J. Wang, *ACS Appl. Energy Mater.*, 2019, **2**, 5363-5372.

14 H.J. Lee, S. Back, J.H. Lee, S.H. Choi, Y. Jung and J.W. Choi, *ACS Catal.*, 2019, **9**, 7099-7108.

15 L. Bai, C.-S. Hsu, D.T.L. Alexander, H.M. Chen and X. Hu, *J. Am. Chem. Soc.*, 2019, **141**, 14190-14199.

16 J. Li, Q. Zhou, C. Zhong, S. Li, Z. Shen, J. Pu, J. Liu, Y. Zhou, H. Zhang and H. Ma, *ACS Catal.*, 2019, **9**, 3878-3887.

17 T. Wen, Y. Zheng, J. Zhang, K. Davey and S.-Z. Qiao, *Adv. Sci.*, 2019, **6**, 1801920.

18 J. Kang, F. Yan, C. Li, L. Qi, B. Geng, Y. Wang, C. Zhu and Y. Chen, *Catal. Sci. Technol.*, 2020, **10**, 6970-6976.

19 X. Zhu, D. Zhang, C.-J. Chen, Q. Zhang, R.-S. Liu, Z. Xia, L. Dai, R. Amal and X. Lu, *Nano Energy*, 2020, **71**, 104597.

20 C. Wang, H. Tong, J. Lu, B. Liu, F. Zheng, W. Tao, W. Zhang and Q. Chen, *Carbon*, 2020, **170**, 414-420.

21 W. Chen, X. Luo, S. Ling, Y. Zhou, B. Shen, T.J.A. Slater, J.A. Fernandes, T. Lin, J. Wang and Y. Shen, *Carbon*, 2020, **168**, 30 588-596.